Characterizing the nuclear models informed by PREX and CREX

Tianqi Zhao (UC Berkeley & Ohio University)
Collaborator: Zidu Lin, Bharat Kumar, Andrew Steiner, Madappa Prakash

INT-24-89W, Aug 26

arXiv.2406.05267

N3AS Network for Neutrinos, Nuclear Astrophysics, and Symmetries
PHYSICS FRONTIER CENTER

NSF

1 8 0 4

OHIO UNIVERSITY

Parity violating electron scattering

	CREX	PREX
(N,Z)	(28,20) Ca	(126,82) Pb
q (fm-1)	0.8733	0.3977
Fch, Rch(fm)	0.1581, 3.481	0.409, 5.503
Apv	2668±106(stat) ±40(syst)	550±16(stat) ±8(syst)
Fw	0.1304±0.0052(stat) ±0.002(syst)	0.368±0.013(exp) ±0.001(theo)
Fch-Fw	0.0277±0.0052(stat) ±0.002(syst)	0.041±0.013(exp) ±0.001(theo)
Rw	3.64±0.026(exp) ±0.023(theo)	5.8±0.075(tot)
Rw-Rch	0.159±0.026(exp) ±0.023(theo)	0.297±0.075(tot)
Rn-Rp	0.121±0.026(exp) ±0.024(theo)	0.283±0.071(tot)

CREX 2022 PREX I 2012 PREX II 2021

MREX: see Tuesday's talk by Concettina

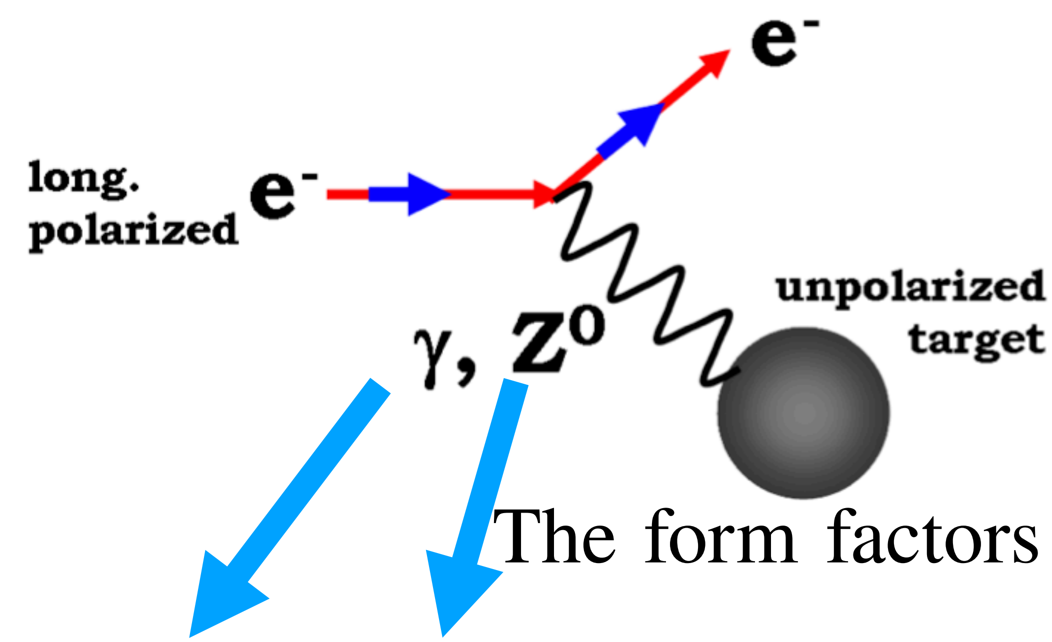

The form factors

$$F_{ch} - F_W = \Delta F$$

The parity violating asymmetry :

$$A_{PV} = \frac{\sigma_R - \sigma_L}{\sigma_R + \sigma_L}$$

The weak interaction violates parity :

$$J_Z^\mu = -\frac{1}{2}\bar{\psi}_L \gamma^\mu \psi_L - \sin^2(\Theta)\bar{\psi}\gamma^\mu \psi$$

Pre PREX-CREX era

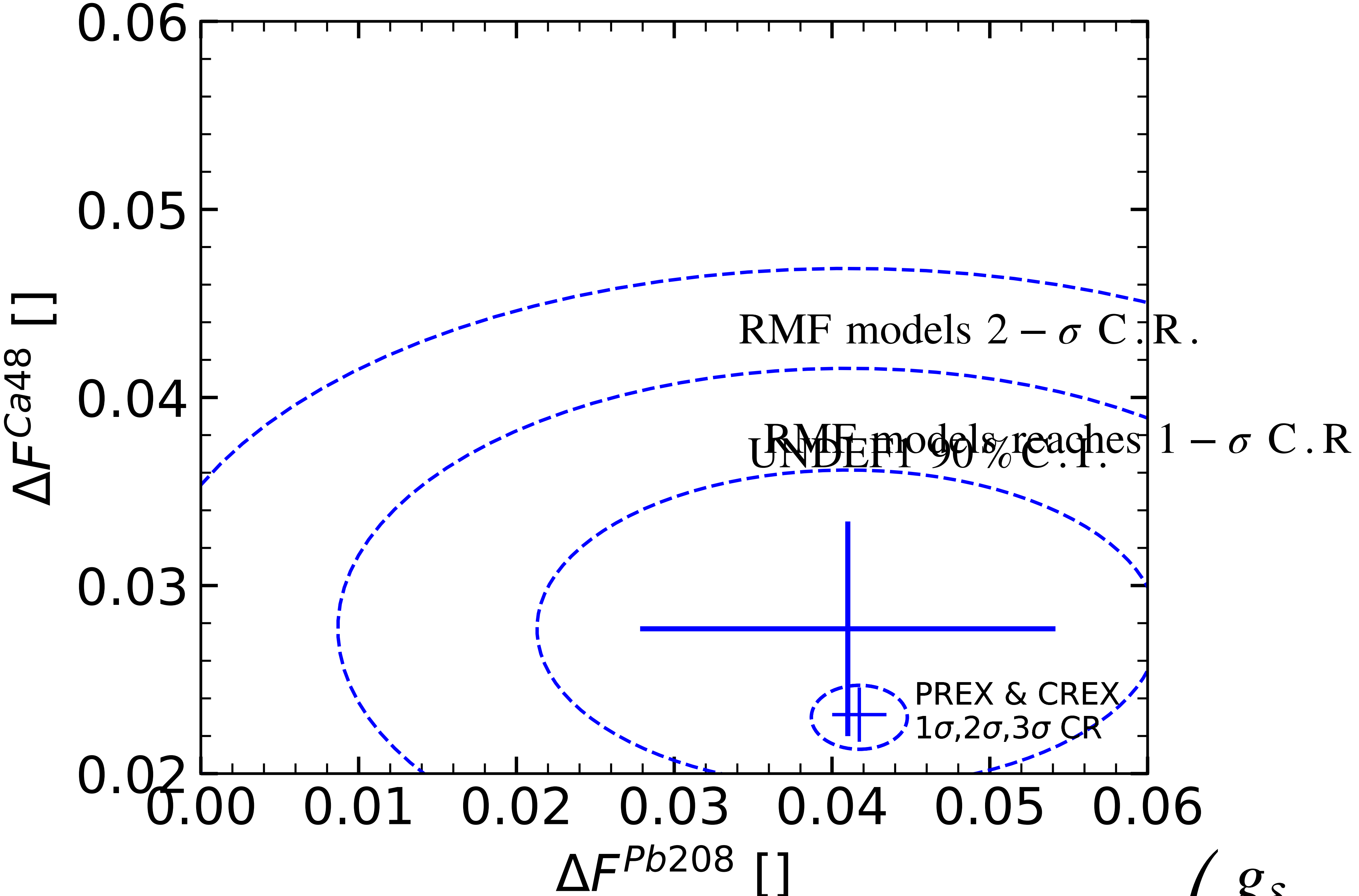

$$\bar{\psi}\left(\frac{g_\delta}{2}\tau\cdot\delta\right)\psi$$

Post PREX-CREX era

- What nuclear properties can we learn from the experiment?
- Why are Skyrme models more compatible than RMF models?
- How may the mean-field model improve in the future?

Skyrme and RMF samples

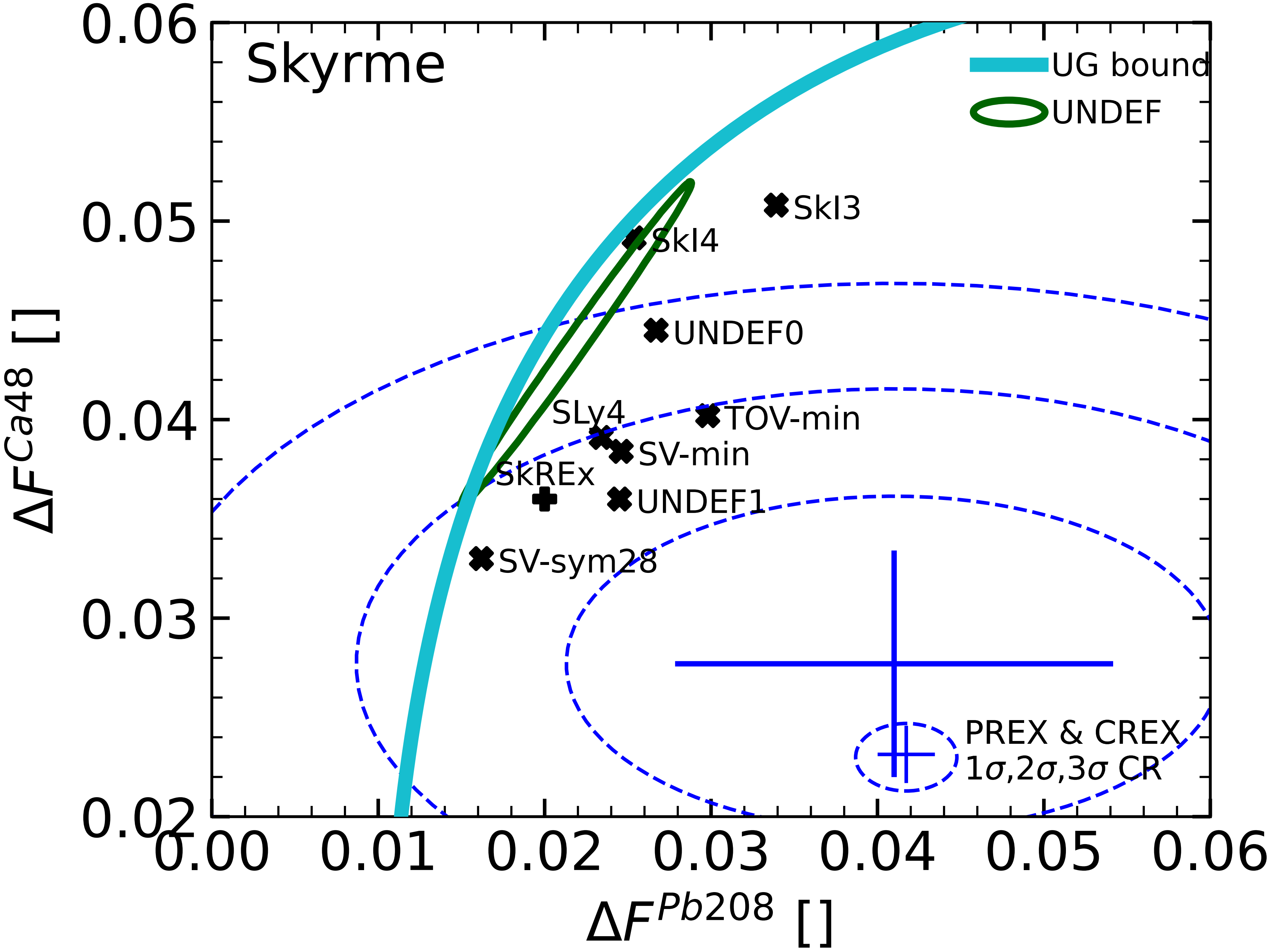

Skyrme models

Symmetry energy S_V

$$S(n) = S_V + \frac{L}{3}\left(\frac{n}{n_S} - 1\right) + \cdots$$

ΔF^{Ca48} and ΔF^{Pb208} are positively correlated for nuclear models with fixed S_V

The correlation is linear:

$S_v = a\Delta F^{Ca48} + b\Delta F^{Pb208} + c$

Fitting parameter for RMF (Skyrme) models:

	a	b	c
RMF	-575.2 ± 5.1	916.3 ± 4.6	32.2 ± 3.7
Skyrme	-503.2 ± 7.8	945.2 ± 5.5	31.9 ± 2.9

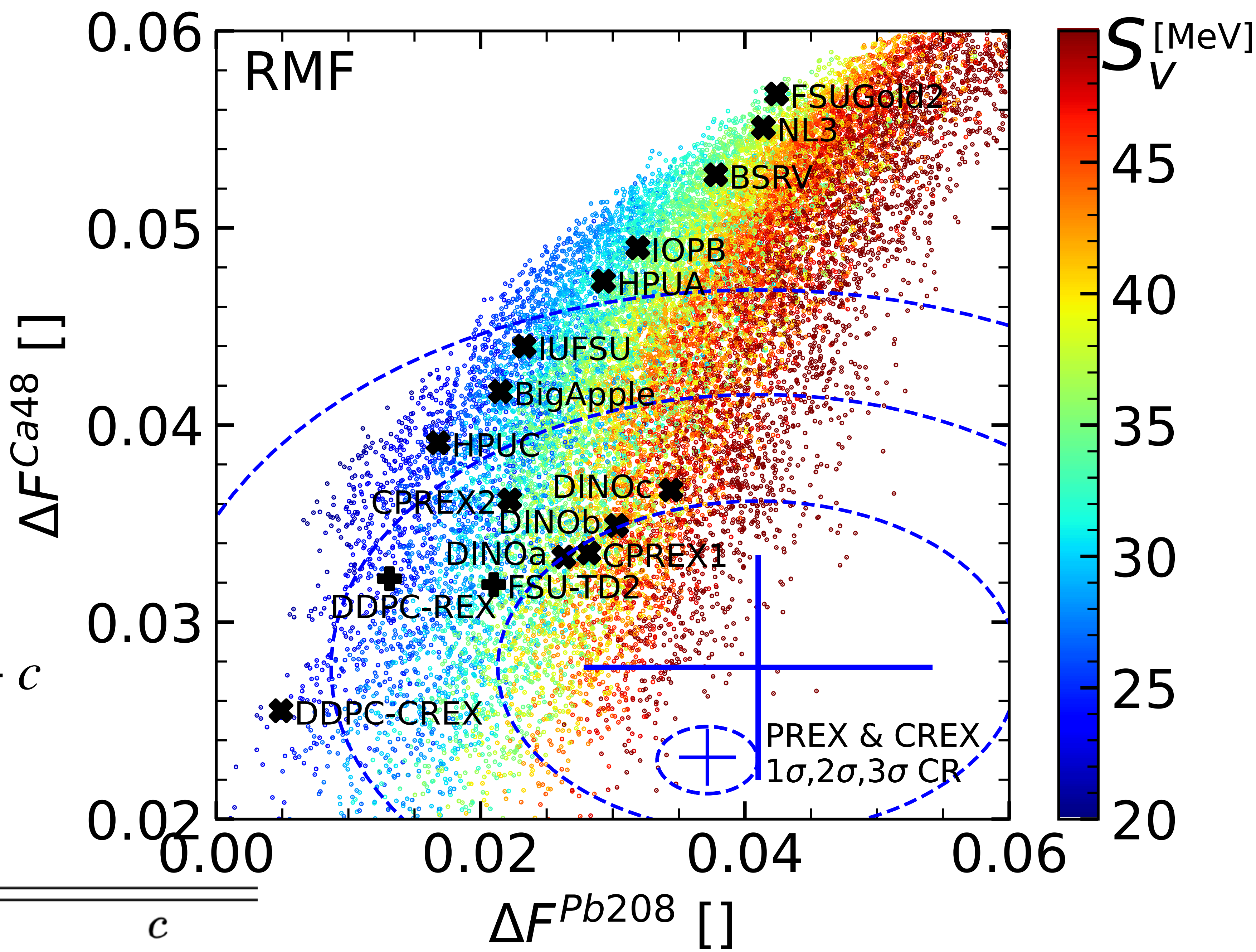

Form factor difference for 48Ca and 208Pb

Symmetry energy slope L

$$S(n) = S_V + \frac{L}{3}\left(\frac{n}{n_S} - 1\right) + \cdots$$

A similar correlation for L has an opposite slope!

The correlation is linear:
$L = a'\Delta F^{Ca48} + b'\Delta F^{Pb208} + c'$

Fitting parameter for RMF (Skyrme) models:

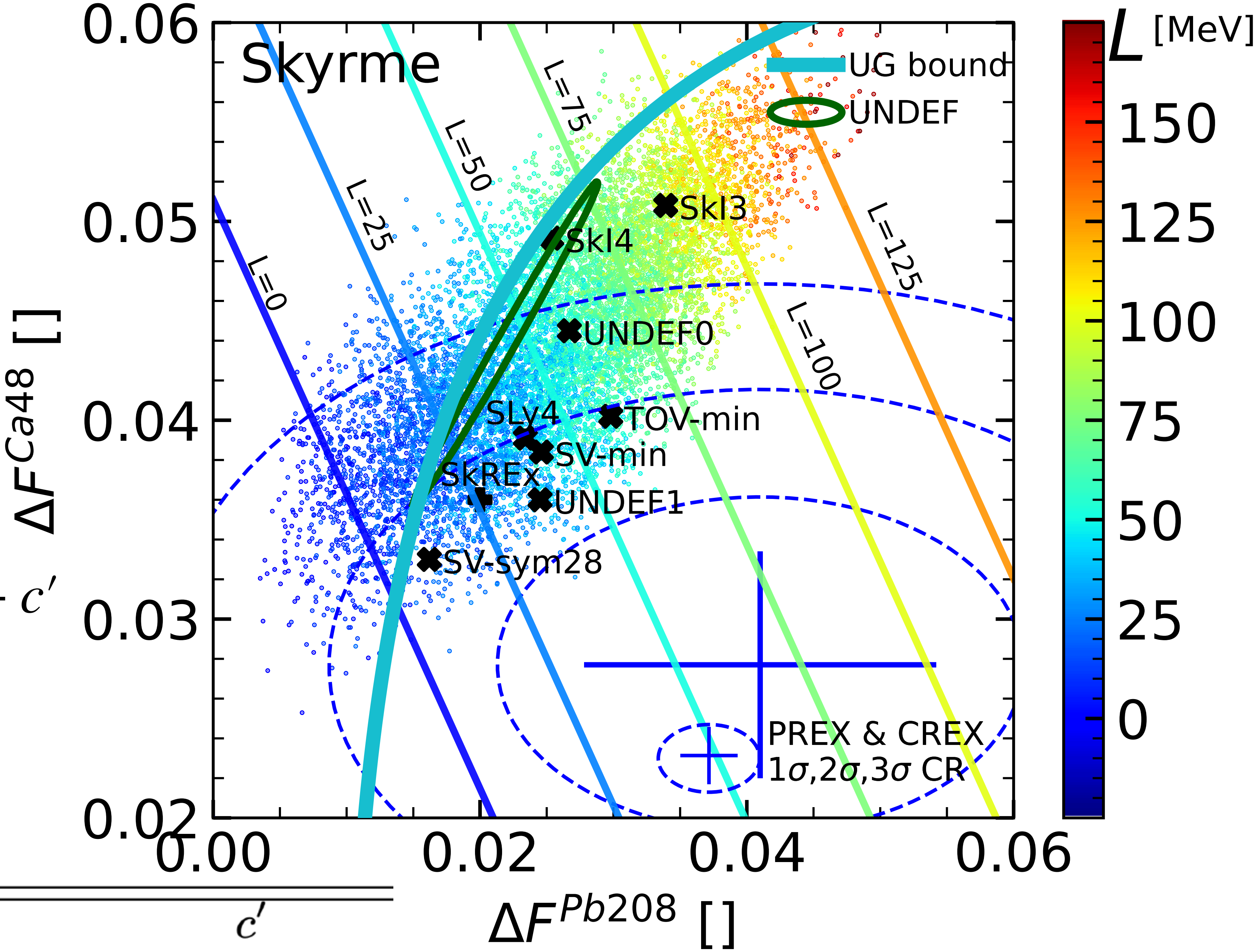

	a'	b'	c'
RMF	2938.7 ± 43.5	2420.6 ± 33.9	-149.8 ± 25.6
Skyrme	1791.2 ± 27.2	2652.0 ± 19.0	-91.5 ± 10.1

Linear correlation of form factor difference

Constraints on (S_V, L) from $(\Delta F^{Ca48}, \Delta F^{Pb208})$

S_V and L can be fixed by ΔF^{Ca48} and(or) ΔF^{Pb208}:

$$S_V = a\Delta F^{Ca48} + b\Delta F^{Pb208} + c$$
$$L = a'\Delta F^{Ca48} + b'\Delta F^{Pb208} + c'$$

PREX:
ΔF^{Pb208}=0.041
±0.013(exp)±0.001(theo)

CREX:
ΔF^{Ca48}=0.0277
±0.0052(stat)±0.002(syst)

PREX+CREX:

$$(\bar{S}_V, \bar{L}) = (56.7,\ 66.8)_{Skyrme}, \quad (53.8,\ 30.9)_{RMF}$$

$$\sqrt{\mathrm{cov}} = \begin{pmatrix} 19.6 & 31.2 \\ 31.2 & 56.5 \end{pmatrix}_{Skyrme}, \quad \begin{pmatrix} 19.5 & 31.0 \\ 31.0 & 66.3 \end{pmatrix}_{RMF}$$

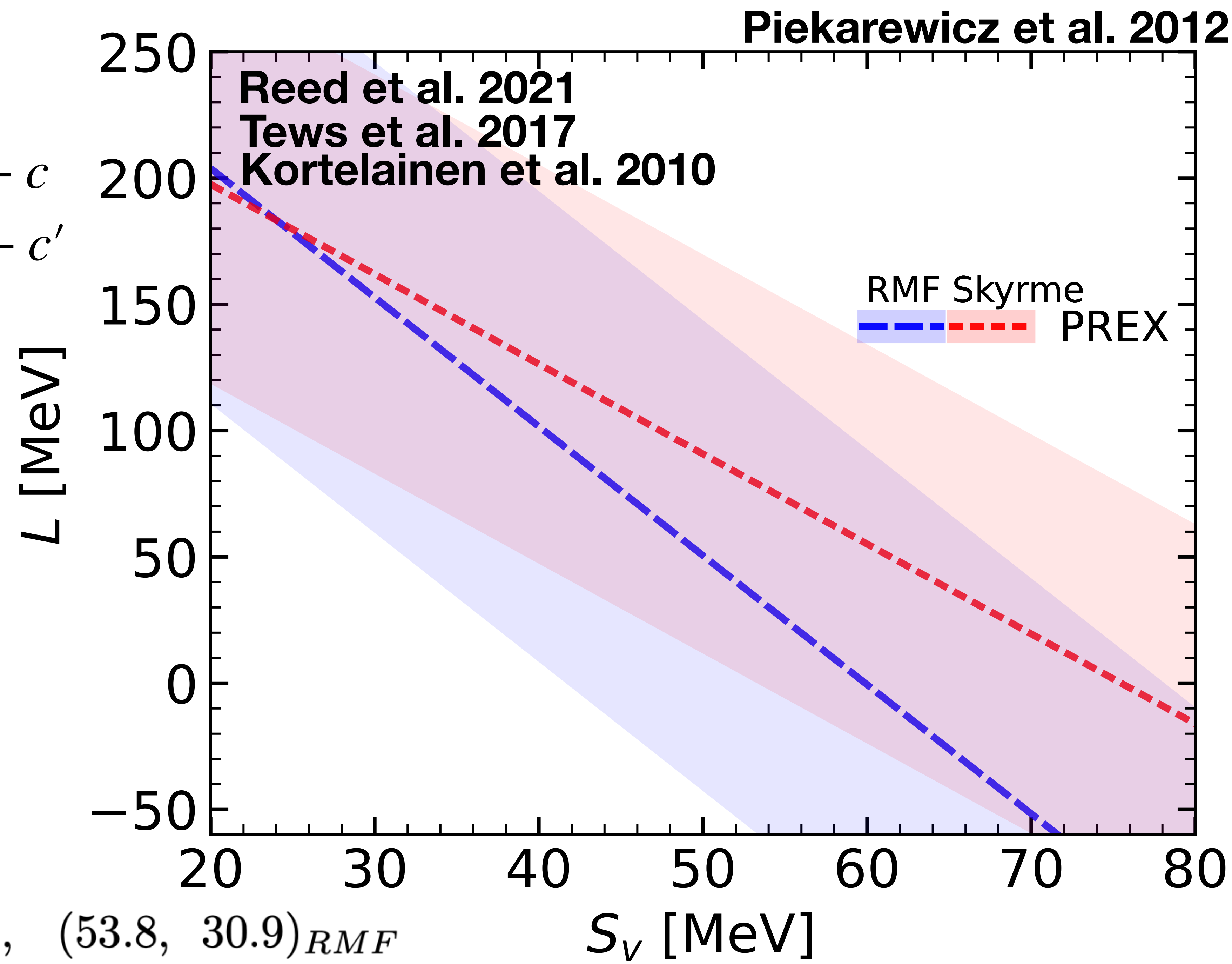

1-sigma band of Sv and L from PREX

Bayesian posterior

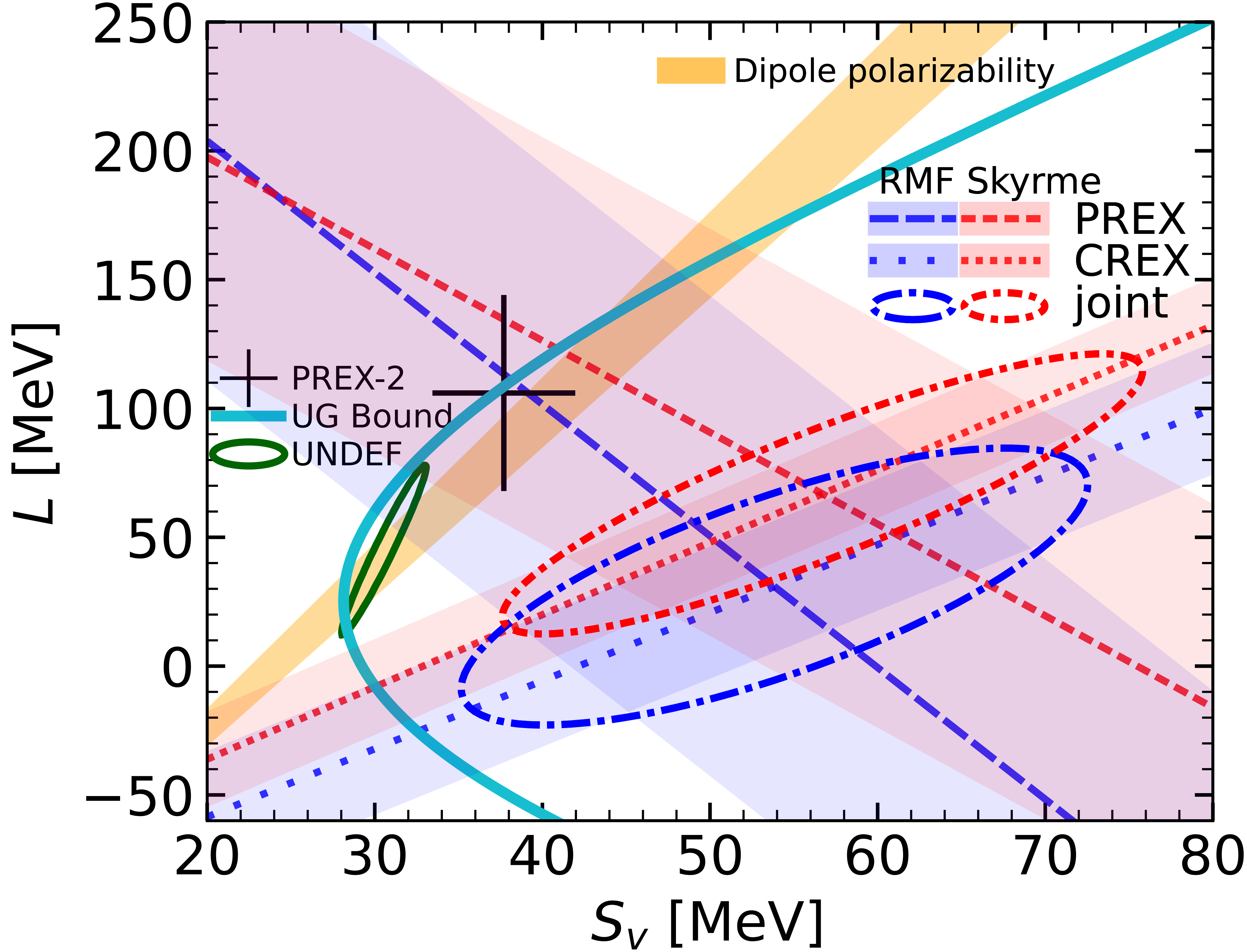

Isovector spin-orbit force

Isovector spin-orbit force is independent of S_V and L in Skyrme (not in RMF) model.

Spin-orbit force in Skyrme model:

$$H_{\rm SO} = b_4 \mathsf{J}\cdot\nabla n + b_4'(\mathsf{J}_n\cdot\nabla n_n + \mathsf{J}_p\cdot\nabla n_p)$$

The freedom b_4' improves the Skyrme model performance.

$v \ll c$ limit of RMF model:

$$b_4' \approx \frac{1}{8m^2}\left(\frac{g_\delta^2}{m_\delta^2} + \frac{g_\rho^2}{m_\rho^2}\right)$$

large δ-meson coupling improves the RMF models.

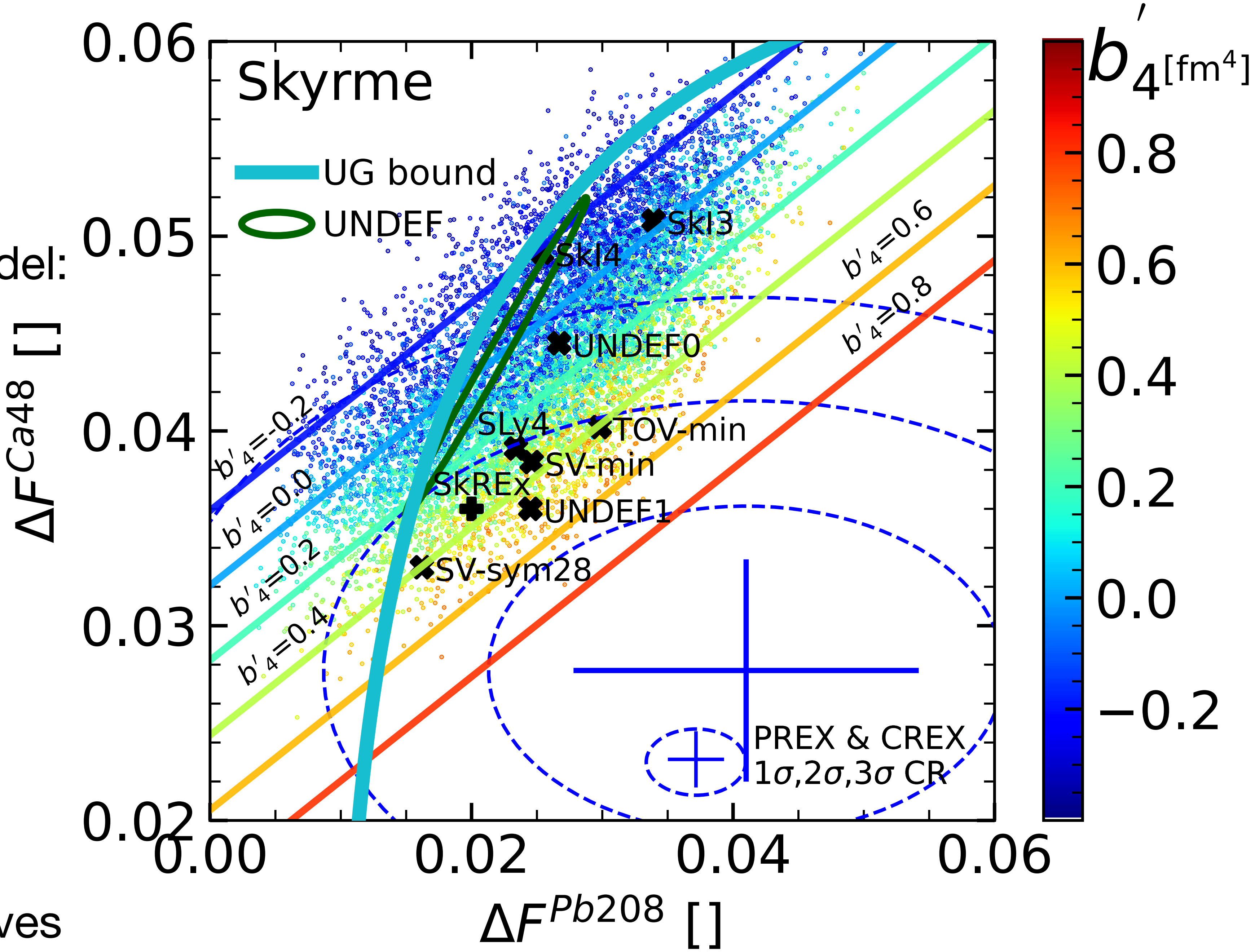

Linear correlation of form factor difference

Impact of b_4' on neutron skin ΔR_{np}

ΔR_{np} of ^{208}Pb increases with b_4'

ΔR_{np} of ^{48}Ca decreases with b_4'

Large b_4' reduces the tension between PREX and CREX.

90% lower bound of b_4':
$b_4' \gtrsim 0.74\ \mathrm{fm}^4$ (Skyrme)
$b_4' \gtrsim 0.54\ \mathrm{fm}^4$ (RMF)

The large density fluctuation inside nuclei may be reduced by introducing addition tensor interactions, see M. Salinas and J. Piekarewicz 2024 (arXiv:2312.13474)

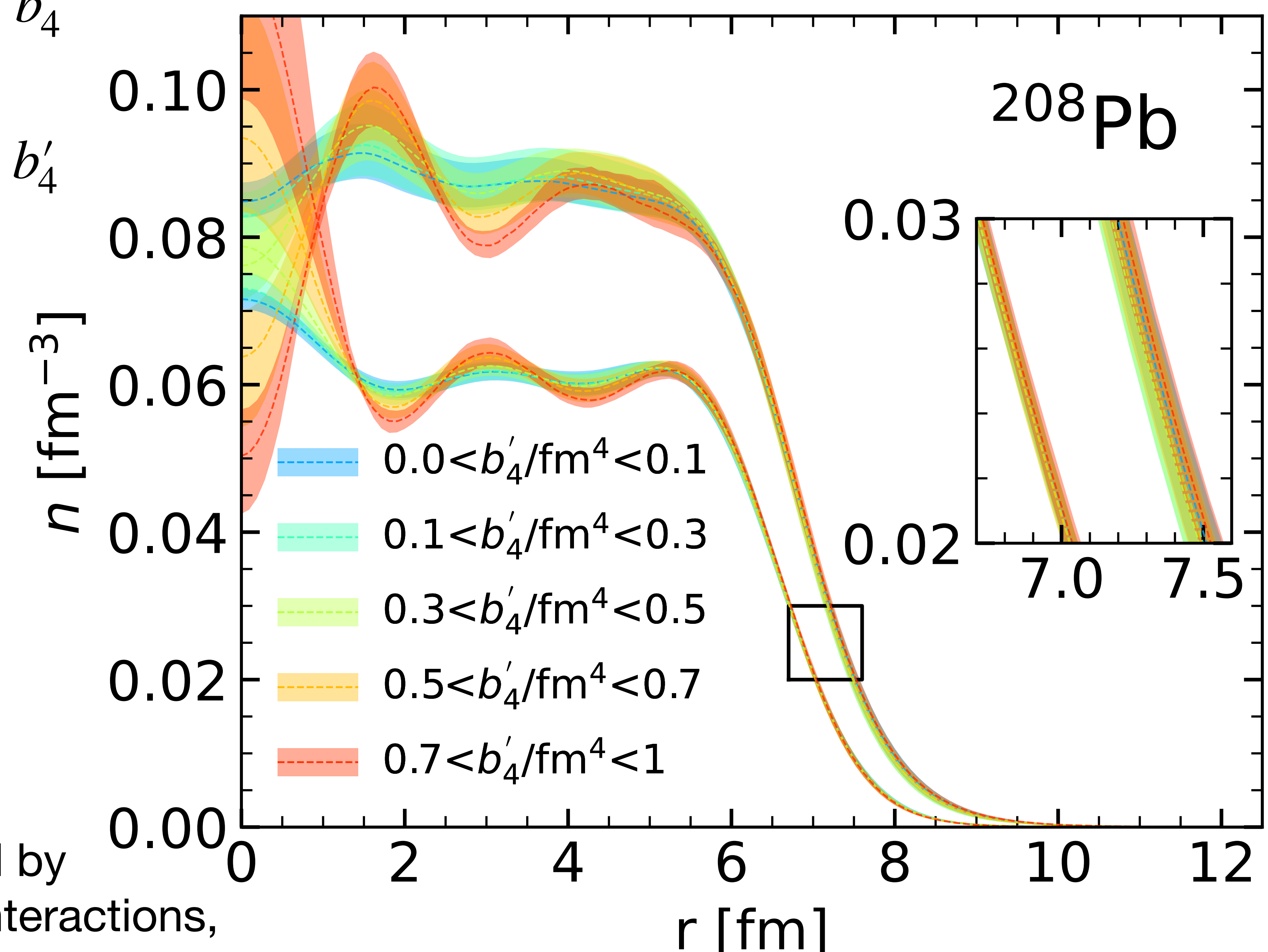

Radial density profile of proton and neutron for 208Pb

Free Tensor Interaction

Spin-orbit force in Skyrme model:
$H_{\rm SO} = b_4 \mathrm{J}\cdot\nabla n$
$+b_4'(\mathrm{J}_n\cdot\nabla n_n + \mathrm{J}_p\cdot\nabla n_p)$
Tensor force in Skyrme model:
$H_{\rm T} = b_J \mathrm{J}^2 + b_J'(\mathrm{J}_n^2 + \mathrm{J}_p^2)$
The freedom b_4', b_4' and b_4'improve the Skyrme model performance, see arXiv.2406.03844:
S240 and eS240: $b_4' = 0.6$ fm^{-4}
S500 and eS500: $b_4' = 1.3$ fm^{-4}

which is consistent with our analysis:
$b_4' = 1.37 \pm 0.49$ fm^{-4}
and 90% lower bound:
$b_4' \gtrsim 0.74\ \mathrm{fm}^4$ (Skyrme)
$b_4' \gtrsim 0.54\ \mathrm{fm}^4$ (RMF)

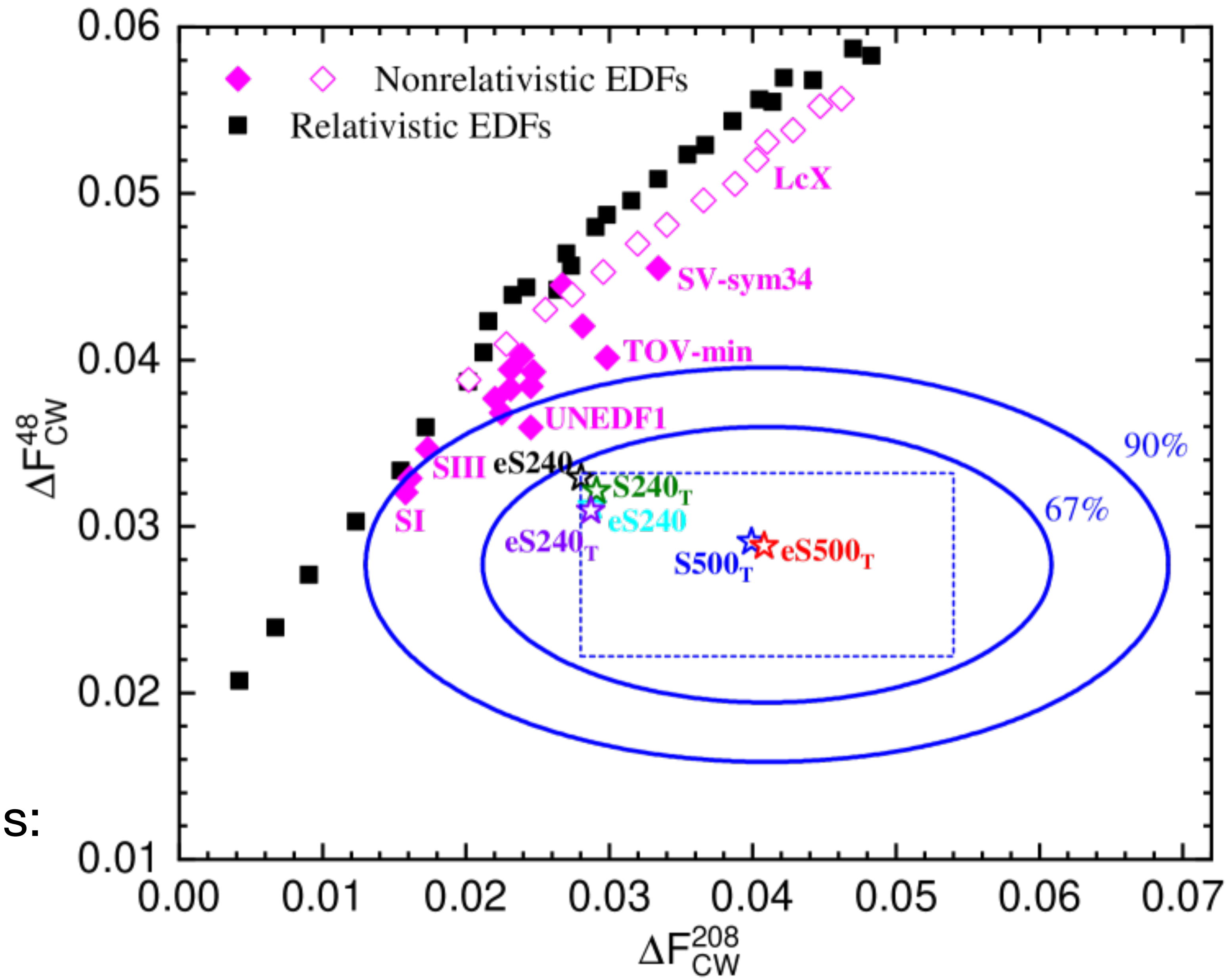

T.G. Yue, Z. Zhang, L.W. Chen arXiv.2406.03844

Post PREX-CREX era

- What nuclear properties can we learn from the experiment?
  PREX+CREX prefers much Larger S_V than expected.

- Why are Skyrme models more compatible than RMF models?
  The freedom in isovector spin-orbit interaction b_4'.

- How may the mean-field model improve in the future?
  Increase the degree of freedom on surface-related isovector interactions, e.g. isovector spin-orbit interaction, isovector tensor interaction.

Thanks to N3AS's support

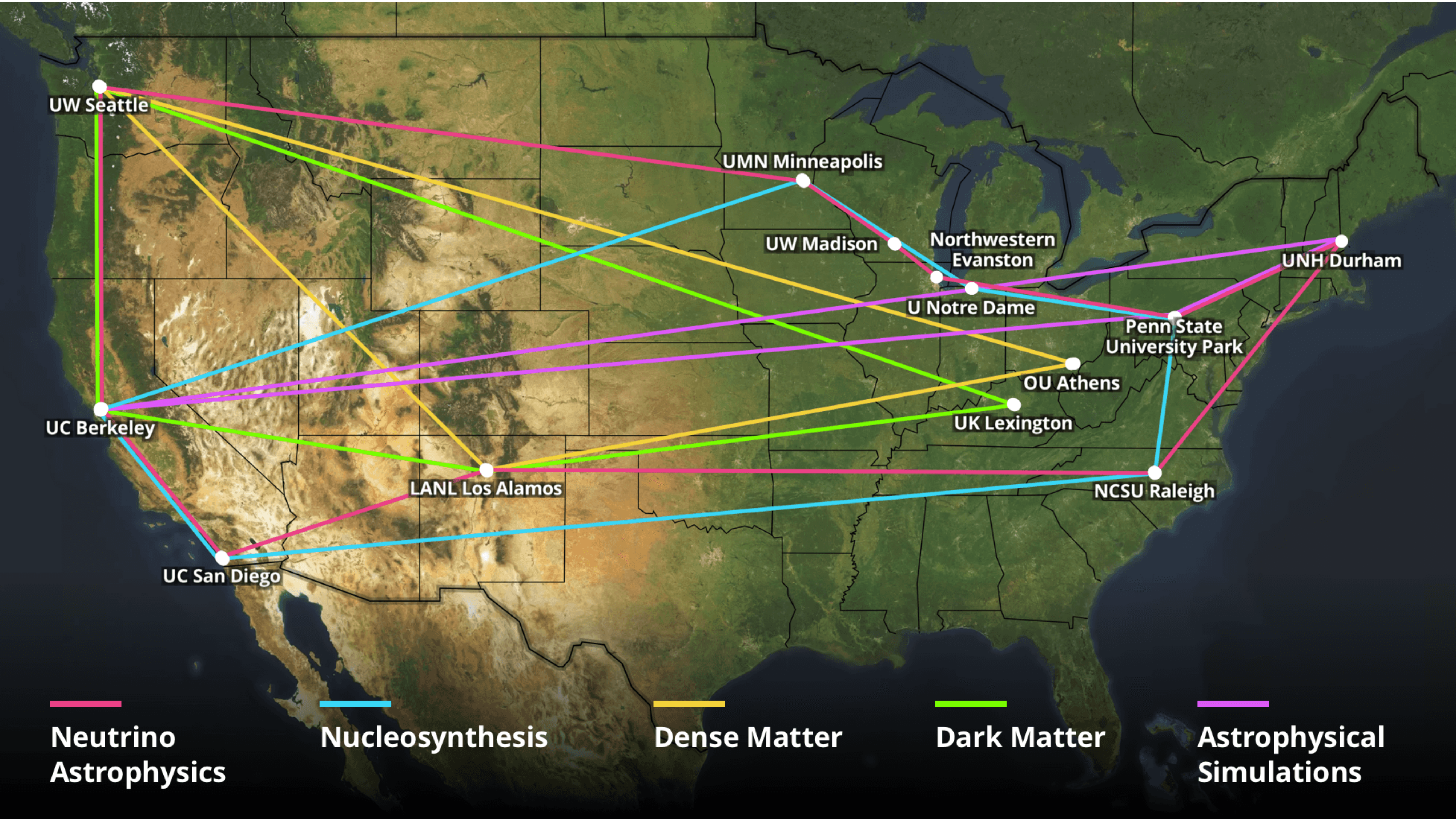

		Experiment	NL3	FSU2	IOPB-I	IUFSU	BigApple	HPUC	BSRV	DINOa	DINOb	DINOc	CPREX1	CPREX2
	B/A [MeV]	7.87	7.88	7.87	7.86	7.88	7.85	7.85	7.84	7.87	7.87	7.87	7.84	7.86
	R_{ch} [fm]	5.50	5.51	5.49	5.52	5.49	5.50	5.56	5.53	5.51	5.51	5.51	5.49	5.49
^{208}**Pb**	ΔR_{np} [fm]	0.159± 0.017	0.2797	0.2862	0.2195	0.1618	0.1508	0.1196	0.2595	0.1746	0.1993	0.2235	0.1905	0.1525
	F_{ch} []	0.409	0.4067	0.4094	0.4052	0.4106	0.4080	0.3992	0.4043	0.4074	0.4075	0.4073	0.4100	0.4092
	ΔF []	0.041±0.013	0.0414	0.0423	0.0319	0.0233	0.0214	0.0168	0.0378	0.0262	0.0303	0.0342	0.0282	0.0222
	B/A [MeV]	8.67	8.65	8.62	8.64	8.53	8.52	8.65	8.66	8.67	8.67	8.67	8.64	8.66
	R_{ch} [fm]	3.48	3.45	3.43	3.45	3.44	3.46	3.46	3.44	3.47	3.47	3.47	3.48	3.46
^{48}**Ca**	ΔR_{np} [fm]	0.137±0.015	0.2255	0.2318	0.1995	0.1736	0.1690	0.1479	0.2196	0.0994	0.1054	0.1141	0.1252	0.1357
	F_{ch} []	0.158	0.1604	0.1665	0.1616	0.1647	0.1582	0.1577	0.1621	0.1591	0.1589	0.1585	0.1537	0.1571
	ΔF []	0.0277±0.0055	0.0551	0.0564	0.0490	0.0435	0.0413	0.0391	0.0527	0.0330	0.0345	0.0364	0.0335	0.0362

TABLE I. Experimental data for the binding energy per nucleon[1], charge radii[2], neutron skins (excluding PREX and CREX)[3], charge from factor and form factor difference from PREX[4] for ^{208}Pb and CREX[5] for ^{48}Ca. Also displayed are the theoretical results obtained with NL3[6], FSUGold2[7], IOPB-I[8], IUFSU[9], BigApple[10], HPUC[11], BSRV[12], DINOa-c[13] and the two new parameterizations, CPREX1 and CPREX2.

		NL3	FSU2	IOPB-I	IUFSU	BigApple	HPUC	BSRV	DINOa	DINOb	DINOc	CPREX1	CPREX2
	n_s [fm^{-3}]	0.1483	0.1504	0.1495	0.1546	0.1546	0.1490	0.1480	0.1522	0.1525	0.1519	0.1516	0.1518
	M^* [MeV]	558.7	557.0	557.2	572.1	572.8	572.9	565.3	587.4	593.0	593.9	692.8	648.1
	B [MeV]	16.24	16.26	16.10	16.40	16.34	15.98	16.10	16.16	16.21	16.21	16.29	16.14
SNM	K [MeV]	271.6	237.7	222.6	231.3	227.0	220.2	227.2	210.0	207.0	206.0	223.8	223.5
	S_V [MeV]	37.3	37.6	33.3	31.3	31.3	28.4	36.1	31.4	33.1	34.6	32.9	29.8
	L [MeV]	118.2	112.7	63.6	47.2	39.8	41.6	84.6	50.0	70.0	90.0	-3.5	0.4
	K_{sym} [MeV]	101.0	25.4	-37.0	28.5	87.5	81.1	-73.2	506.0	609.1	714.8	-418.4	-239.8
	M_n^* [MeV]	569.2	566.0	566.7	580.5	582.8	581.4	573.3	352.1	333.0	320.5	377.4	465.6
	M_p^* [MeV]	569.2	566.0	566.7	580.5	582.8	581.4	574.8	908.8	948.2	969.1	1062.5	870.1
PNM	S_V [MeV]	38.3	38.6	34.7	32.9	33.1	29.9	37.2	46.5	50.6	53.4	54.3	38.4
	L [MeV]	121.2	115.9	67.7	49.5	40.6	42.7	88.7	172.1	216.4	247.8	211.2	75.9
	K_{sym} [MeV]	100.3	27.2	-45.5	23.1	74.3	89.2	-70.6	726.7	907.2	1021.2	801.8	76.4
	M_{max} [$M_\odot$]	2.77	2.07	2.15	1.94	2.60	2.05	2.04	2.17	2.15	2.15	2.04	2.12
	$R_{1.0}$ [km]	14.4	14.1	13.2	12.6	12.8	12.6	13.6	14.4	14.8	15.1	13.9	12.9
NS	$R_{1.4}$ [km]	14.5	13.9	13.2	12.6	13.1	12.8	13.4	14.4	14.6	14.9	13.4	12.9
	$\Lambda_{1.0}$ []	7797	6473	4347	3384	3918	3752	4903	6623	7572	8579	4543	3544
	$\Lambda_{1.4}$ []	1275	876	687	500	719	593	689	1065	1150	1256	584	570

TABLE II. Saturation properties and neutron star properties of RMF models listed in Table I. Saturation properties for SNM and PNM are defined in the letter. Neutron star properties are calculated with the crust EOSs constructed with the compressible liquid droplet model repectively for various RMF models with fixed surface tension parameters $\sigma_s = 1.2$ MeV fm^{-2}, $S_S = 48$ MeV[14].

Neutron star EOS

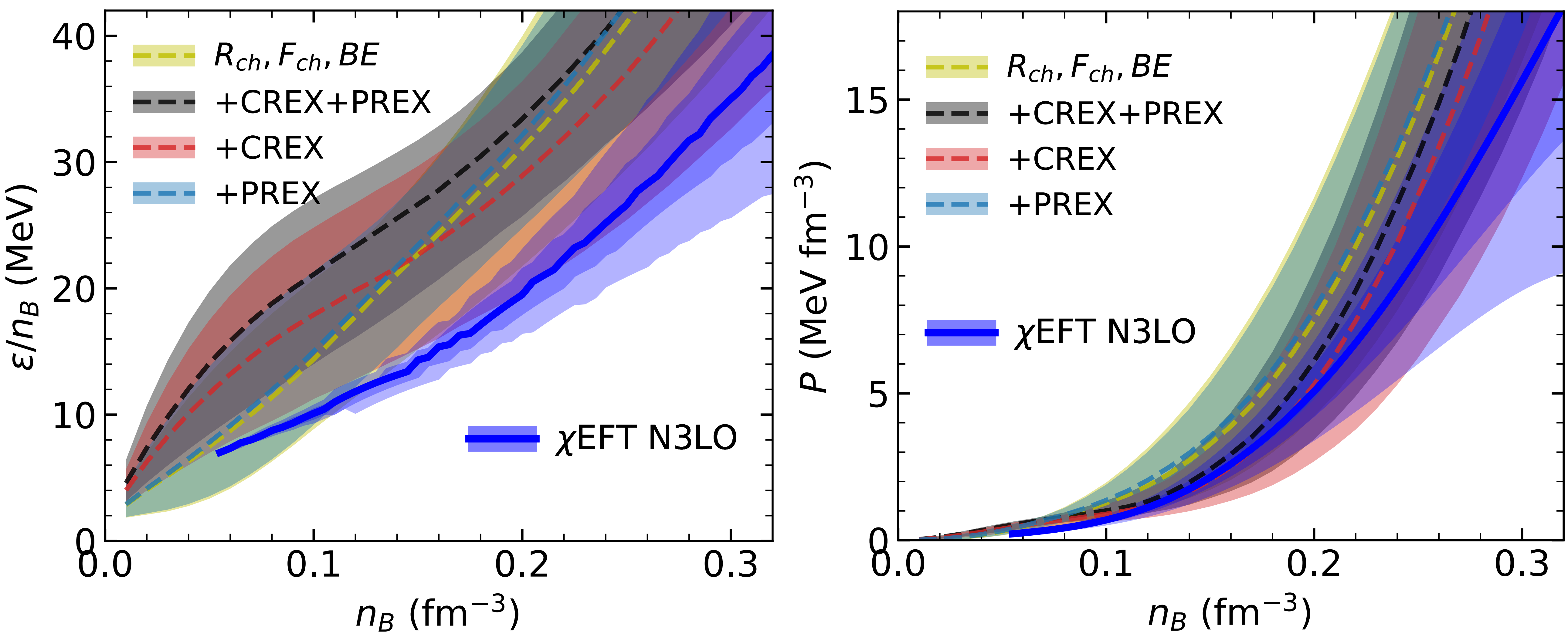

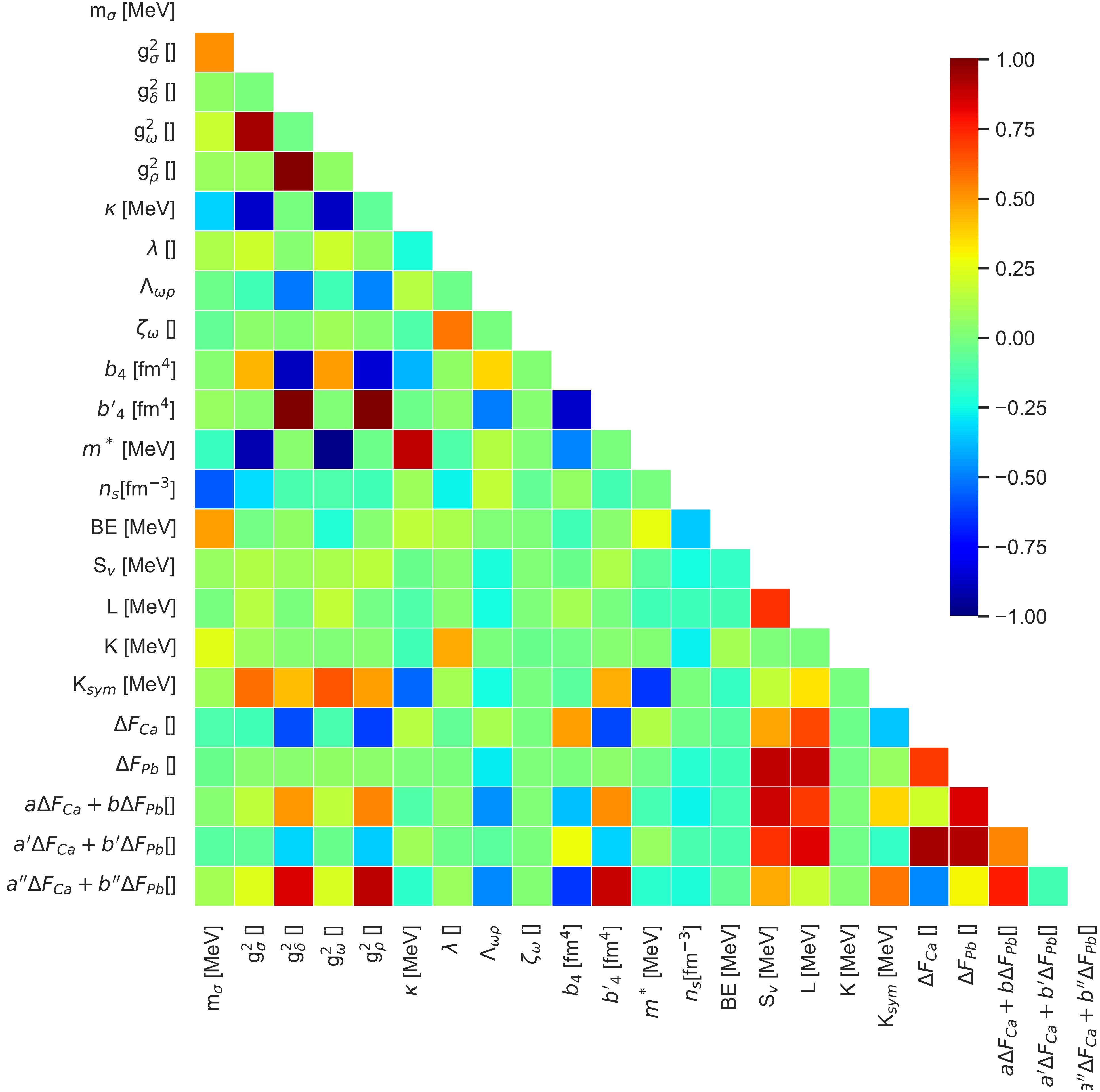

m_σ [MeV]
g_σ^2 []
g_δ^2 []
g_ω^2 []
g_ρ^2 []
κ [MeV]
λ []
$\Lambda_{\omega\rho}$
ζ_ω []
b_4 [fm^4]
b'_4 [fm^4]
m^* [MeV]
n_s[fm^{-3}]
BE [MeV]
S_v [MeV]
L [MeV]
K [MeV]
K_{sym} [MeV]
ΔF_{Ca} []
ΔF_{Pb} []
$a\Delta F_{Ca} + b\Delta F_{Pb}$[]
$a'\Delta F_{Ca} + b'\Delta F_{Pb}$[]
$a''\Delta F_{Ca} + b''\Delta F_{Pb}$[]
1.00
0.75
0.50
0.25
0.00
−0.25
−0.50
−0.75
−1.00

RMF

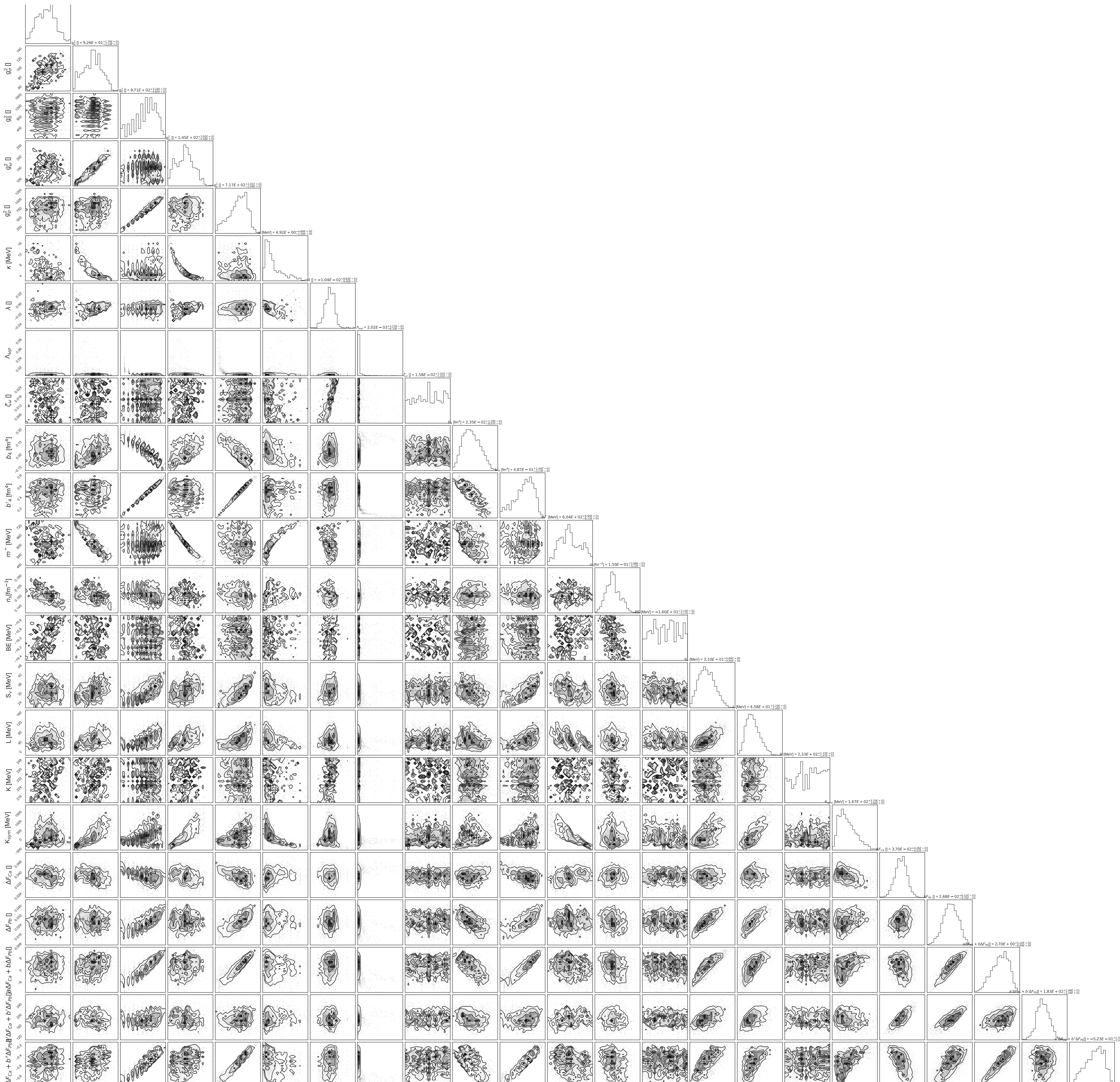

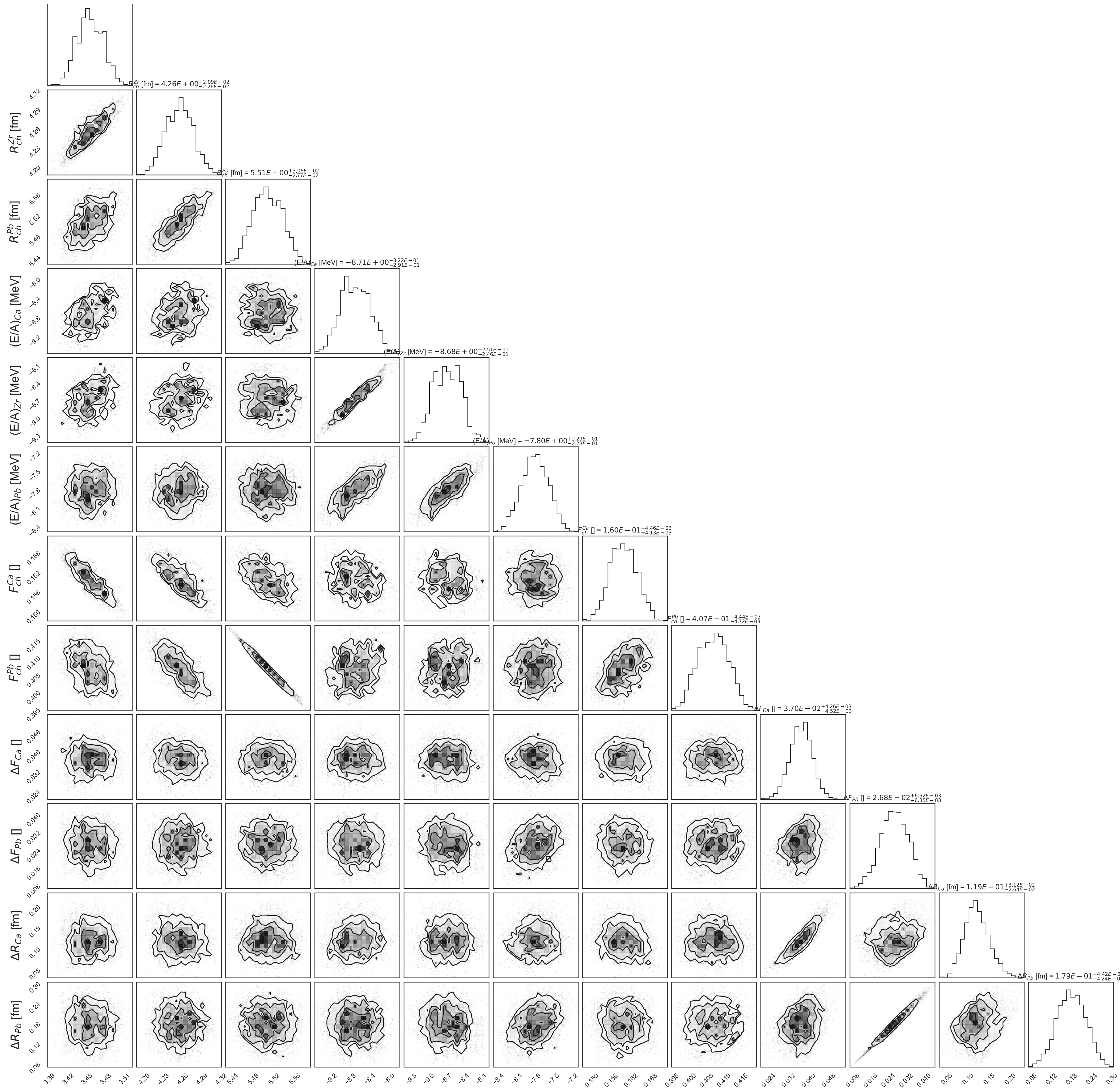

R_{ch}^{Zr} [fm] = $4.26E+00^{+2.09E-02}_{-2.26E-02}$
R_{ch}^{Pb} [fm] = $5.51E+00^{+3.06E-02}_{-2.77E-02}$
$(E/A)_{Ca}$ [MeV] = $-8.71E+00^{+3.22E-01}_{-2.91E-01}$
$(E/A)_{Zr}$ [MeV] = $-8.68E+00^{+2.51E-01}_{-2.46E-01}$
$(E/A)_{Pb}$ [MeV] = $-7.80E+00^{+2.29E-01}_{-2.23E-01}$
F_{ch}^{Ca} [] = $1.60E-01^{+4.46E-03}_{-4.13E-03}$
F_{ch}^{Pb} [] = $4.07E-01^{+4.44E-03}_{-4.72E-03}$
ΔF_{Ca} [] = $3.70E-02^{+4.26E-03}_{-4.52E-03}$
ΔF_{Pb} [] = $2.68E-02^{+6.52E-03}_{-6.35E-03}$
ΔR_{Ca} [fm] = $1.19E-01^{+3.12E-02}_{-2.64E-02}$
ΔR_{Pb} [fm] = $1.79E-01^{+4.42E-02}_{-4.24E-02}$
R_{ch}^{Zr} [fm]
R_{ch}^{Pb} [fm]
(E/A)$_{Ca}$ [MeV]
(E/A)$_{Zr}$ [MeV]
(E/A)$_{Pb}$ [MeV]
F_{ch}^{Ca} []
F_{ch}^{Pb} []
ΔF_{Ca} []
ΔF_{Pb} []
ΔR_{Ca} [fm]
ΔR_{Pb} [fm]

RMF